



## THERMOMECHANICAL CHARACTERIZATION OF THE COMPLEX STIFFNESS OF A SHAPE MEMORY ALLOY HELICAL SPRING

**Samuell Aquino Holanda**

**Antonio Almeida Silva**

Universidade Federal de Campina Grande, Rua Aprígio Veloso, 882, Bairro Univeritário, Campina Grande, Paraíba, Brazil.  
samuell182@gmail.com, almeida@dem.ufcg.edu.br

**Alberdan Santiago de Aquino**

Instituto Federal da Paraíba, Avenida Primeiro de Maio, 720, Bairro Jaguaribe, João Pessoa, Paraíba, Brazil.  
alberdan@ifpb.edu.br

**Carlos José de Araújo**

Universidade Federal de Campina Grande, Rua Aprígio Veloso, 882, Bairro Univeritário, Campina Grande, Paraíba, Brazil.  
carlos@dem.ufcg.edu.br

**Rômulo do Nascimento Rodrigues**

Universidade Federal de Campina Grande, Rua Aprígio Veloso, 882, Bairro Univeritário, Campina Grande, Paraíba, Brazil.  
eng.romulorodrigues@gmail.com

**Aureliano Xavier dos Santos**

Universidade Federal de Campina Grande, Rua Aprígio Veloso, 882, Bairro Univeritário, Campina Grande, Paraíba, Brazil.  
aureliano@yahoo.com.br

**Abstract.** Shape memory alloys (SMA) are being increasingly used for the development of smart actuators because of their unique thermomechanical properties. Many of the applications for these SMA actuators consider the possibility of force generation and applications in confined spaces. A SMA spring actuator becomes important when it is necessary higher displacements and moderate lifting capacity loads. This paper investigate the thermomechanical behavior and properties of a spring made of NiTi SMA wire, emphasizing the determination of the complex stiffness of the NiTi wire related with properties of storage modulus and loss factor. The NiTi SMA spring actuator was studied using thermal analysis (DSC and DMA), mechanical cycling under constant temperature and assembled in a mass-spring system for the analysis of free vibration responses. A set of data as phase-transformation temperatures, thermal hysteresis, stiffness, damping and finally the complex stiffness that characterizes the SMA actuator were obtained.

**Keywords:** *Thermomechanical behavior, SMA helical spring, Complex stiffness*

### 1. INTRODUCTION

Currently, the scientific development in the field of vibration control requires the application of actuators and sensors technologically more advanced than the conventional ones. These advanced sensors and actuators can be related to the use of materials classified as "smart" that can change its properties when subjected to certain external forces. As an example of these smart materials, shape memory alloys (SMA) can modify their mechanical properties with temperature.

SMA can be used to manufacture efficient thermomechanical actuators for many applications, as for example, the control of mechanical vibrations. Thus, it is necessary to explore the potential of SMA in developing systems for vibration control that are more efficient than conventional solutions, through changes in the natural frequency of the structure and the consequent reduction in the amplitude of vibrations.

At the same time that the variation of stiffness, the damping behavior of the mechanical system incorporating a SMA actuator also change with the variation of temperature. In general, SMA are classified as metallic materials with high damping capacity, mainly due to its hysteretic behavior related to phase transformations into the material during heating and cooling.

However, the behavior of these SMA is nonlinear, which makes its modeling a more complex task, which requires further thermomechanical analysis to determine intrinsic characteristics such as complex stiffness, which considers the energy dissipation per cycle and frequency dependence that cause variations in structural damping (Inman, 2000).

In this paper, the thermomechanical behavior of a SMA helical spring is studied. For the characterization of the SMA material it were performed thermal analysis (DSC and DMA) of the NiTi wire selected to manufacture the coil spring and a mass-spring system of one degree of freedom was employed for the analysis of dynamic response of the SMA spring.

## 2. SHAPE MEMORY ALLOY ACTUATORS

SMA materials have the unusual ability to recover its original shape by heating after being pseudo plastically deformed by external forces. During solid state phase transformation by heating and cooling, these smart metals may exhibit significant variation in the elastic modulus and damping characteristics. Therefore, mechanical components manufacture with SMA can be integrated into the design of actuators and structures in order to improve increase and control their static and dynamic characteristics (Yuvaraja and Kumar, 2012; Gupta, 2000; Liang and Rogers, 1993).

In addition to the variations in stiffness, SMA have high damping properties that are associated with changes in crystalline structure during phase transformation. This high damping is attributed to the dissipation of energy into these SMA. Due to its reversible deformation, high tensile strength as well as excellent fatigue resistance, SMA has been studied for damping control in applications involving active and passive vibration attenuation (Chang and Wu, 2007).

In this work, for simulation of the stiffness variation as a function of temperature in a SMA spring and validate the experimental test it was used the Ikuta's model (1991) as proposed by Aquino (2011). Equations (1) and (2) represent, respectively, the stiffness ( $k$ ) of a SMA actuator during heating and cooling.

$$k_{SMA-A} = k_{min} + \left( (k_{max} - k_{min}) - \frac{(k_{max} - k_{min})}{1 + e^{\left(\frac{6,2}{A_F - A_S} \left(T \frac{A_F + A_S}{2}\right)\right)}} \right) \quad (1)$$

$$k_{SMA-M} = k_{min} + \left( (k_{max} - k_{min}) - \frac{(k_{max} - k_{min})}{1 + e^{\left(\frac{6,2}{M_S - M_F} \left(T \frac{M_F + M_S}{2}\right)\right)}} \right) \quad (2)$$

where:

$k_{SMA-A}$ :	Spring stiffness during heating;
$k_{SMA-M}$ :	Spring stiffness during cooling;
$k_{min}$ :	Minimum Stiffness;
$k_{max}$ :	Maximum Stiffness;
$M_S$ :	Martensite starts temperature;
$M_F$ :	Martensite finish temperature;
$A_S$ :	Austenite start temperature;
$A_F$ :	Austenite finish temperature;
$T$ :	Temperature of the SMA spring;

## 3. COMPLEX STIFFNESS

Considering a system of one degree of freedom, as pointed out in Fig. (1), the force required to impose a displacement  $x$  is given by:

$$F = kx + c\dot{x} \quad (3)$$

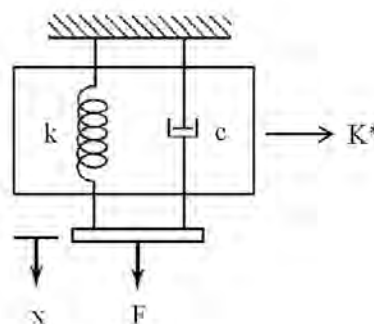


Figure 1. Schematic representation of complex stiffness of a SMA actuator.

Assuming a harmonic motion of the type  $x = Xe^{i\omega t}$ , the force is given by:

$$F = kXe^{i\omega t} + ic\omega Xe^{i\omega t} \quad (4)$$

$$F = (k + i\omega c)x \quad (5)$$

From Eq. (5) one arrives at the concept of complex stiffness:

$$k(1 + i \frac{c\omega}{k}) \quad (6)$$

$$k^* = k(1 + i\eta) \quad (7)$$

Here  $\eta$  is called the loss factor and  $k^*$  is defined as the complex stiffness. This formulation regards the damping of the system as a component of complex stiffness. The imaginary part of the complex stiffness,  $i\eta$ , corresponds to the energy dissipated in the system because the loss factor can be written as follows:

$$\eta = \frac{c\omega}{k} \quad (8)$$

One way to determine the loss factor of the material is adopt the equivalent viscous damping factor  $\zeta_{eq}$ , which can be obtained by (Inman, 2000):

$$\delta \cong 2\pi\zeta_{eq} \cong \pi\eta \quad (9)$$

$$\zeta_{eq} \cong \frac{\eta}{2} \quad (10)$$

From Eq. (10) it is possible obtain the equivalent relationship between the equivalent damping factor  $\zeta_{eq}$  and loss factor  $\eta$ :

$$\eta \cong 2\zeta_{eq} \quad (11)$$

#### 4. THERMOMECHANICAL CHARACTERIZATION OF THE SMA WIRE

For this work it was selected a NiTi SMA wire with 2.02 mm in diameter. To eliminate some of the strain hardening of the supplied material, the SMA wire was annealed at 400°C for 30 minutes and cooled at room temperature. After this heat treatment, two samples were removed indicated in Tab. (1).

Table 1 – NiTi SMA sample sizes.

	Sample 1	Sample 2
Length	1,5 mm	31,2 mm
Weight	0,0065 g	0,663 g

Sample 1 was used to determine the phase transformation temperatures of the SMA NiTi wire by DSC (Differential Scanning Calorimetry). For this measurement was used a DSC calorimeter (TA Instruments, model Q20). The test was performed with a heating and cooling rate of 5°C/min and a temperature range between 0°C and 100°C. Figure (2) shows the characteristic behavior obtained from the DSC.

HOLANDA, S.A., ALMEIDA, A.A., AQUINO, A.S., ARAÚJO, C.J., RODRIGUES, R.N., SANTOS, A.X.  
**Thermomechanical Characterization of the Complex Stiffness in a SMA Helical Spring**

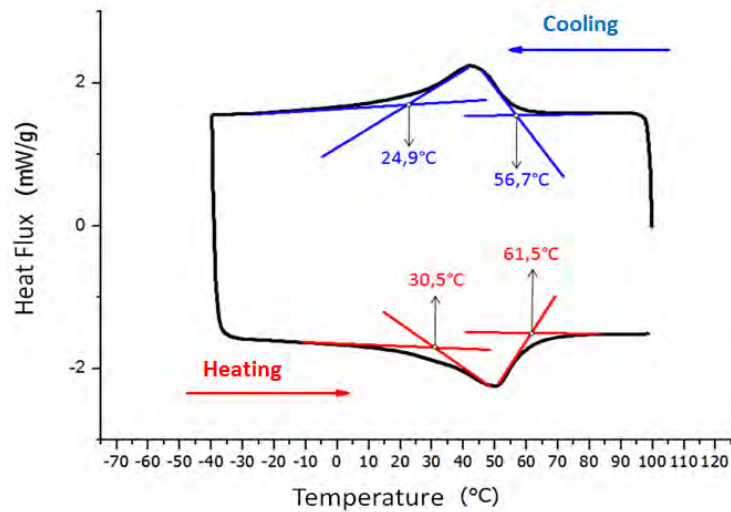


Figure 2. Transformation temperatures of the NiTi SMA wire obtained by DSC.

The phase transformation temperatures were:  $M_s=56.7^\circ\text{C}$  (martensite start),  $M_f=24.9^\circ\text{C}$  (martensite finish),  $A_s=30.5^\circ\text{C}$  (austenite start) and  $A_f=61.5^\circ\text{C}$  (austenite finish). Comparing the two temperatures of the DSC peaks, it can be verified that this SMA NiTi has a low thermal hysteresis, of the order of  $H_T = 8^\circ\text{C}$ .

In parallel, two analyzes of dynamic behavior was performed with sample 2 using a Dynamic Mechanical Analyzer (DMA, model Q800, TA Instruments) in order to observe the influence of the excitation frequency and temperature on the behavior of the elasticity modulus and loss factor.

For the first test the sample 2 was tested in the DMA at three different temperatures ( $30^\circ\text{C}$ ,  $50^\circ\text{C}$  and  $70^\circ\text{C}$ ) corresponding to regions with different crystalline phases (martensite, mixture and austenite). The experiments were carried out in a single cantilever beam mode by applying a tip force with variable oscillating frequency (8 a 150 Hz) corresponding to a constant amplitude deflection of  $5\ \mu\text{m}$ . The results of these DMA tests are shown in Figs. (3) and (4).

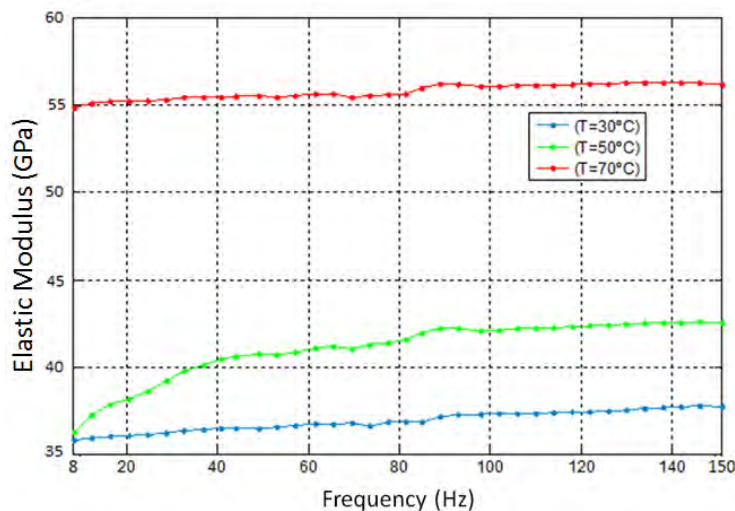


Figure 3. Elastic modulus versus frequency for the NiTi SMA wire at three different temperatures:  $30^\circ\text{C}$ ,  $50^\circ\text{C}$  e  $70^\circ\text{C}$ .

The increase of temperature change significantly the elastic modulus, which showed values of about 36 GPa ( $30^\circ\text{C}$ ), 41 GPa ( $50^\circ\text{C}$ ) e 55 GPa ( $70^\circ\text{C}$ ), taking as reference the frequency of 80 Hz. The behavior of elastic modulus as a function of frequency showed small variations, mainly for the martensitic ( $30^\circ\text{C}$ ) and austenitic ( $70^\circ\text{C}$ ) stable states, with a tendency to stabilize above 100 Hz.

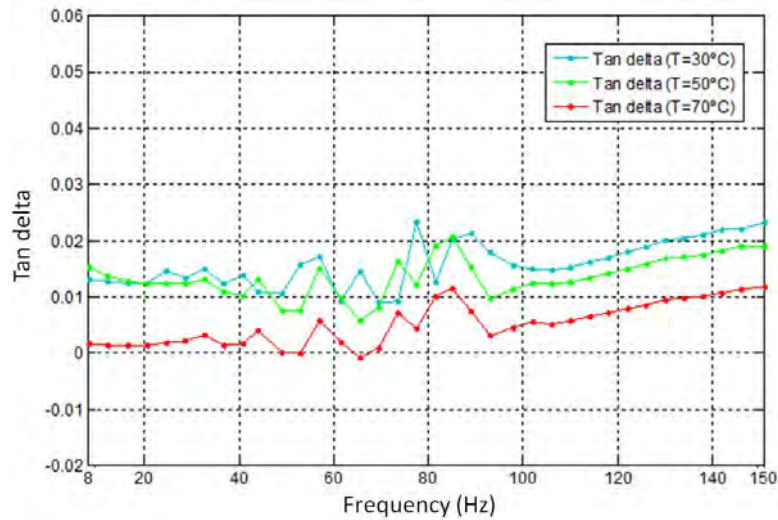


Figure 4. Loss factor versus frequency for the NiTi SMA wire at 30°C, 50°C e 70°C.

The behavior of the loss factor was the inverse of the elastic modulus as pointed out in Fig. (4). A reduction in the measured values with increasing temperature was verified. The damping in the austenitic phase (70°C) is smaller than the values found in the martensitic phase (30°C). It was observed a variation of the loss factor as a function of frequency with a tendency to increase linearly for frequencies above 100 Hz.

The second experiment performed on sample 2 was realized to analyze the influence of the frequency on the stiffness (elastic modulus) and damping ( $\text{Tan}\delta$ ) from a range of temperature starting at 25°C until 100°C, for four different frequencies (1 Hz, 5 Hz, 10 Hz e 12 Hz).

Figures (5) and (6) show the characteristic curves obtained from these DMA analyses. The behavior of elastic modulus not suffers much influence of the frequency variations, being more dependent of the test temperature. For example, in the martensitic state (30°C) the elastic modulus increases of about 3 GPa between 1 Hz and 12 Hz. However, Fig. (5) show a considerable increase in elastic modulus for all frequencies along the phase transformation during heating. This increase of elastic modulus with temperature indicates a corresponding increase in the stiffness of the SMA material, resulting in less energy dissipation at high temperatures by the structure.

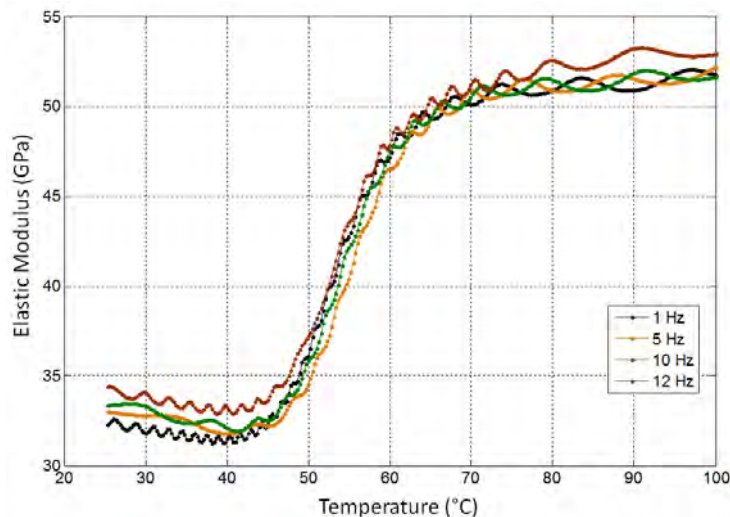


Figure 5. Behavior of the elastic modulus with the change of excitation frequency

Figure (6) shows the behavior of the loss factor as a function of temperature and frequency. It is observed that the highest peaks of loss factor appear during the phase transformation for the lowest frequency (1 Hz). Higher excitation frequencies tend to inhibit the  $\text{Tan}\delta$  peaks, so that for frequencies higher than 5 Hz peak values decrease rapidly.

HOLANDA, S.A., ALMEIDA, A.A., AQUINO, A.S., ARAÚJO, C.J., RODRIGUES, R.N., SANTOS, A.X.  
**Thermomechanical Characterization of the Complex Stiffness in a SMA Helical Spring**

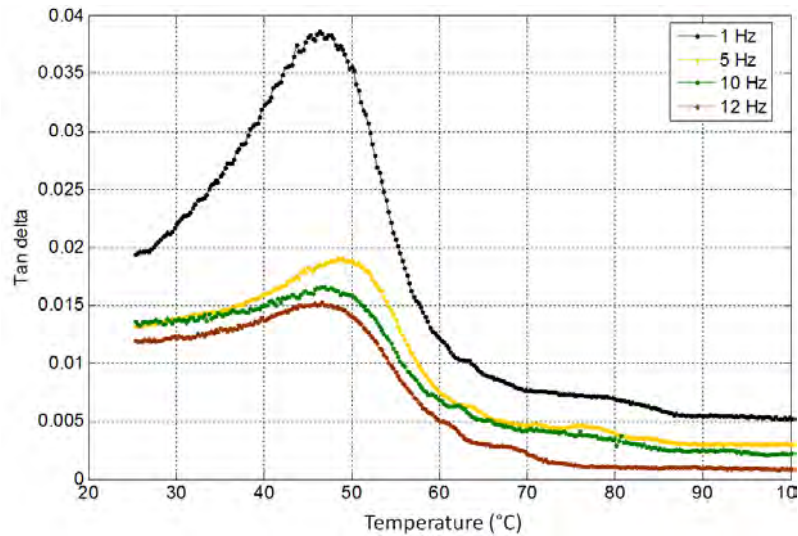


Figure 6. Behavior of the loss factor with the change of excitation frequency

The variation of stiffness and damping observed in Figs. (5) and (6) are related to the internal movements of martensite variants into the material structure, with lower stiffness and high damping in the martensitic phase as compared to austenitic phase (Otsuka and Wayman, 1998).

## 5. FABRICATION AND THERMOMECHANICAL CHARACTERIZATION OF THE SMA HELICAL SPRING

Figure (7) show the SMA helical spring manufactured from the selected NiTi SMA wire. The manufacturing process involves winding the NiTi wire around a guide screw with subsequent heat treatment at 400°C for 30 minutes to obtain the final shape of coil spring. The spring design parameters can be verified in Table (2).



Figure 7. SMA helical spring.

Table 2. Parameters of the SMA helical spring.

Material	NiTi SMA
Wire diameter	2,02 mm
Mean diameter	12,00 mm
Pitch	4,61 mm
Number of active coils	7

As pointed out in Fig. (5), SMA show changes in the elastic modulus from a thermal loading. Therefore, the behavior of the stiffness of the NiTi SMA spring showed in Fig. (7) was studied from a theoretical and experimental point of view.

For determining the SMA spring stiffness during heating and cooling it was used a universal testing machine INSTRON 5582 equipped with a controlled heating chamber.

For this one, the spring was subjected to five cycles of compression loading and unloading, with 10 mm of maximum deflection in a temperature range between 25°C and 70°C, in steps of 5°C. Figure (8) shows the superposition of experimental and theoretical results for the SMA spring stiffness. The theoretical behavior was calculated using Ikuta model, as described in equations (1) e (2).

From these curves it is observed that the stiffness increased 1.37 times at the end of heating when compared with the initial value at 25°C. For temperatures higher than 60°C the stiffness tends to stabilize, due to the fact that from this point the crystalline structure of the SMA spring is fully austenitic. Similarly, it can be predicted stabilization for stiffness at temperatures below 25°C when the SMA is fully martensitic.

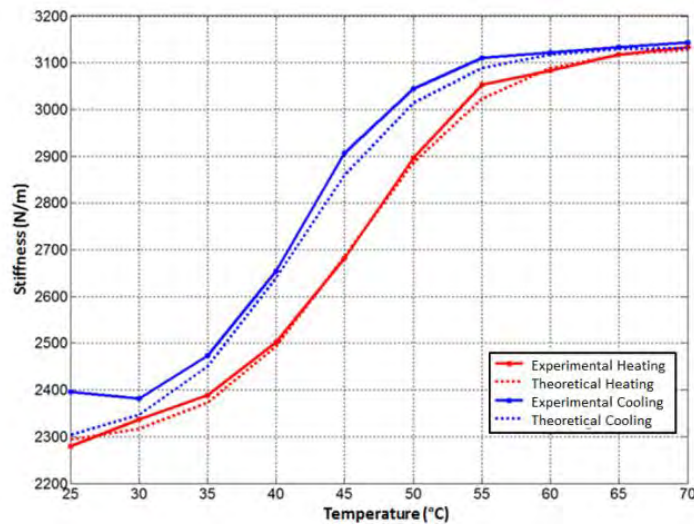


Figure 8. Theoretical and experimental stiffness of the NiTi SMA spring as a function of temperature

Comparing Figures (5) and (8) it is observed similar behaviors of pure elastic modulus of the NiTi SMA and stiffness of the smart spring as a function of temperature.

To calculate the equivalent damping factor, the response of a one degree of freedom system in free vibration after given impulse input through an impact hammer was studied. From this experiment was possible to obtain a curve that characterizes the decay of the displacements with time (Fig. (9)) and applied the method of logarithmic decrement, calculating the ratio between two chosen signal amplitudes.

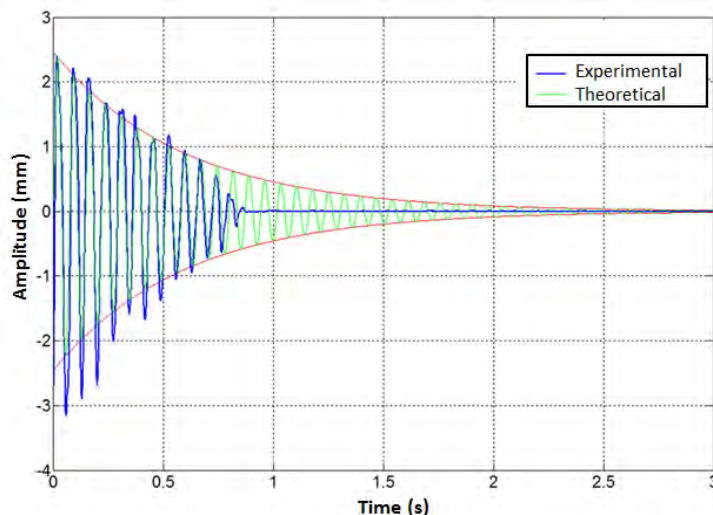


Figure 9. Impulse response (Spring Temperature 70°C)

Thus it was possible to obtain the behavior of damping factor of the SMA spring during heating and cooling, as shown in Fig. (10).

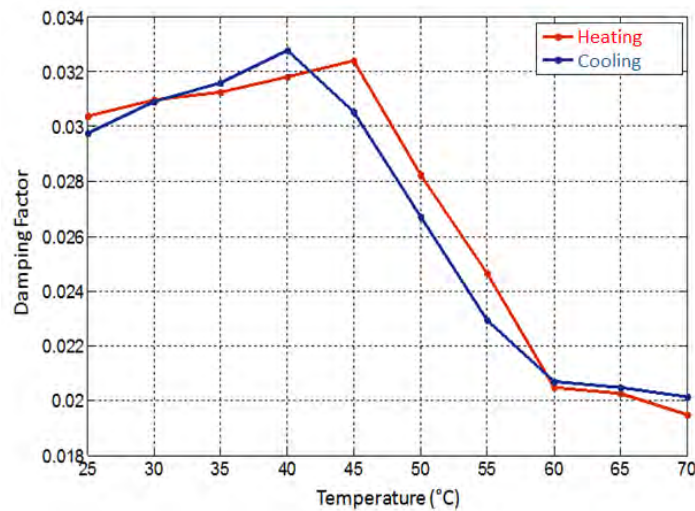


Figure 10 Damping factor of the SMA spring as a function of temperature.

From Figure (10), it can be observed damping peaks during phase transformation of the SMA spring, in the range between 40°C and 45°C, where the corresponding damping factors calculated were, respectively, 0.03277 e 0.03241 for the two mentioned temperatures. The minimum damping factor was found in the austenitic phase (70°C), equal to 0.01947. Already in the martensitic phase, the highest damping factor calculated was 0.03037. The qualitative behavior of the damping factor shown in Fig. (10) is similar to the one of  $\tan \delta$  for the SMA wire measured in the DMA, as pointed out in Fig. (6). The damping peak found during phase transformation is observed mainly due to the transient character of this region, which is related to accommodation of austenite-martensite variants during thermally induced transformation.

Table (3) allows to verify the validity of the relationship between the loss factor and the damping factor,  $\eta = 2\zeta$ . As this relationship is valid only when the system is in resonance, the loss factor of the NiTi SMA spring was calculated from the simplification of Eq. (12). Considering the ratio of frequency equal to 1, Eq. (13) is obtained. The damping factors used was those corresponding to the  $k$  values obtained in Fig. (8).

$$X = \frac{F_0/k}{\sqrt{(1-r^2)^2 + (2\zeta r)^2}} \quad (12)$$

$$\eta = \frac{F_0/k}{X} \quad (13)$$

Therefore, it is possible to validate the relationship between the loss factor and the damping factor defined by Eq. (11). In this case, it was verified errors below of 12%.

Table 3. Relationship between damping factor and loss factor for the resonance condition.

Temperature (°C)	2*Damping factor ( $2\zeta eq$ )	Loss factor $\eta$
25	0,06074	0,07204
30	0,06192	0,07265
35	0,06248	0,07529
40	0,06358	0,07643
45	0,06482	0,07635
50	0,05646	0,05988
55	0,0493	0,05043
60	0,04096	0,04268
65	0,04054	0,03810
70	0,03894	0,03385

## 6. CONCLUSIONS

This paper investigated the thermomechanical characterization of a SMA helical spring, considering only the NiTi SMA wire and further when the manufactured SMA spring is incorporated at one degree of freedom system. The main conclusions that can be outlined from the obtained results are presented below.

- The elastic modulus showed a of the NiTi SMA wire increase slightly with frequency. Furthermore, the modulus increases significantly during phase transformations, verifying the influence of growing temperature. It was observed approximately 60% of increase in this property when comparing the values of the martensitic phase with the austenitic phase;
- During the DMA analysis it has been observed that increasing the excitation frequency of the SMA wire leads to a decay of the damping capacity,  $\tan \delta$ , much due to decreased mobility in the crystalline structure. The SMA wire showed the lowest  $\tan \delta$  in the austenitic phase region and greatest value in the phase transformation region, although the damping capacity of the martensitic region is also high and most used, since it does not depend on the kinetic energy generated by the phase change;
- The results of experimental SMA spring stiffness showed good agreement with the behavior estimated by the theoretical model proposed by Ikuta *et al* (1991). The stiffness of the SMA spring at the austenitic phase (hot) became about 1.37 times higher than the one of the martensitic phase (cool);
- The damping factor of the 1 DOF system measured experimentally also behaved as expected, showing the maximum value at the martensitic region (cool) and a minimum at the austenitic phase (hot). The behavior of the damping is the opposite of the stiffness and each of these parameters interfere differently on the dynamic response of the mechanical system.

## 7. ACKNOWLEDGEMENTS

The authors thank the CAPES Brazilian Agency for the MSc scholarship of the first author and the CNPq for funding the following research projects: INCT of Smart Structures for Engineering (Project 574001/2008-5), Casadinho UFCG-UFRJ-ITA (Project 552199/2011-7) and Universal 14/2011 (Project 472771/2011-6).

## 8. REFERENCES

- AQUINO, A.S. Controle de Vibração de um Sistema sob Desbalanceamento Rotativo Utilizando Atuador de Liga com Memória de Forma. *Thesis (Engenharia Mecânica)* – Universidade Federal da Paraíba, 2011.
- CHANG, S.H.; WU, S.K. Internal Friction of R-Phase and B19 Martensite In Equiatomic TiNi Shape Memory Alloy Under Isothermal Conditions. *Journal of Alloys and Compounds*, v. 438, p. 120-126, 2007.
- GUPTA, K. Critical Speed Analysis of Fibre Reinforced Composite Rotor Embedded with Shape Memory Alloys Wires. *International Journal of Rotating Machinery*, v. 6, n. 3, p. 201-213, 2000.
- HOLANDA, S.A. Estudo da Rigidez Complexa de um Sistema Vibratório Incorporando Atuador Memória de Forma. *Dissertation (Engenharia Mecânica)* – Universidade Federal de Campina Grande, 2013.
- IKUTA, K.; HIROSE, S.; TSUKAMOTO, M. Mathematical Model and Experimental Verification of Shape Memory Alloy for Designing Microactuator. *Proceedings of the 1991 IEEE MicroElectralMechanical Systems Conference*, pp. 103-108, 1991.
- INMAN, D.J. *Engineering Vibration*. 2<sup>a</sup> ed. Prentice Hall, 2000.
- LIANG, C.; ROGERS, C. A. Design of Shape Memory Alloys Springs with Applications in Vibration Control. *Journal of Sound and Vibration and Acoustics*, v. 115, p. 129-135, 1993.
- OTSUKA, K.; WAYMAN, C.M.; *Shape Memory Materials*. 1<sup>a</sup> ed. Cambridge University: New York, 1998.
- YUVARAJA, M.; KUMAR, M.S.; Experimental Studies on SMA Spring Based Dynamic Vibration Absorber for Active Vibration Control. *European Journal of Scientific Research*, v. 77, n.2, p. 240-251, 2012.

## 9. RESPONSIBILITY NOTICE

The authors are the only responsible for the printed material included in this paper.